Article

Dynamic Analysis for the Hydraulic Leg Power of a Powered Roof Support

Dawid Szurgacz [1,2]

1   Center of Hydraulics DOH Ltd., 41-906 Bytom, Poland; dawidszurgacz@vp.pl
2   Polska Grupa Górnicza S.A., 40-039 Katowice, Poland

Abstract: This paper presents the results of a study conducted to determine the dynamic power of a hydraulic leg. The hydraulic leg is the basic element that maintains the position of a powered roof support. It is located in the structure between the canopy and the floor base. The analysis assumes that its power must be greater than the energy of the impact of the rock mass. The energy of the rock mass is generated by tremors caused mainly by mining exploitation. The mining and geological structure of the rocks surrounding the longwall complex also have an influence on this energy generation. For this purpose, stationary tests of the powered roof support were carried out. The analysis refers to the space under the piston of the leg, which is filled with fluid at a given pressure. The bench test involved spreading the leg in the test station under a specified pressure. It was assumed that the acquisition of dynamic power would be at the point of pressure and increase in the space under the piston of the leg under forced loading. Based on the experimental studies carried out, an assessment was made with the assumptions of the methodology adopted. The results of the theoretical analysis showed consistency with the experimental results.

Keywords: power; powered roof support; hydraulic leg; bench testing; dynamic load

1. Introduction

One of the main problems associated with underground coal mining is descending depth. Therefore, the exploitation of coal deposits requires the mining industry to conduct research on technology development [1] and the monitoring of work parameters [2–6] in order to improve the safety of crews [6–9]. The development of mining determines the need for experimental [10–13] and theoretical [14–18] work, aimed at a deeper understanding and analysis of the influence of various factors and the relationships between them. Research into the dynamic loading of roof support defined future directions in [19], and it was shown, among other things, which forces are generated by the pressure on the test leg. This resulted in the theoretical identification of the parameters of susceptible shoring for gallery workings [20].

Ongoing testing of hydraulic legs under mass impact loading is intended to determine the actual resistance of the leg to dynamic loading [21–23]. The dynamic load resistance of a hydraulic leg is understood as the capacity to absorb the energy of a mass impact over a well-defined period of time without breaking or being damaged. Dynamic tests of hydraulic legs allow the assessment of their suitability for use in tremor hazard conditions [24–27]. The weight of the impactor mass used in the tests is assumed to be approximately 1/10th of the working support of the leg. Making this assumption allows for the technical implementation of the research. In mass impact studies, we relate its value to the support of a model-type leg with a constant rate of hydraulic fluid pressure build-up [28–30].

The dynamic load on a powered roof support is caused by the movement of the rock mass, causing energy to be transferred from the rock mass to the powered roof support. These loads occur during short-term tremors. The tremor-causing centres are usually thick sandstone banks located in the roof or the bottom of the mine workings [31].

Among the dynamic phenomena occurring in mines, a distinction is made between tremors, stress relief, and rockbursts. A tremor is a seismic phenomenon that manifests itself in mines by vibration of the rock mass and acoustic effects. In the case of strong tremors, the vibrations of the rock mass is felt at the surface. The relaxation of the rock mass manifests itself through its vibration, acoustic effects, and the cracking of the rock around the excavation. The phenomenon is combined with minimal slides of the support and minor damage, which does not reduce the functionality of the excavation. A rockburst causes rocks to be thrown into the excavation, vibrating the rock mass. A rockburst is usually accompanied by damage or destruction of the support and subsequent clamping and collapse of the workings [32]. Legs that are not designed to take dynamic loads are most likely to be damaged (Figure 1).
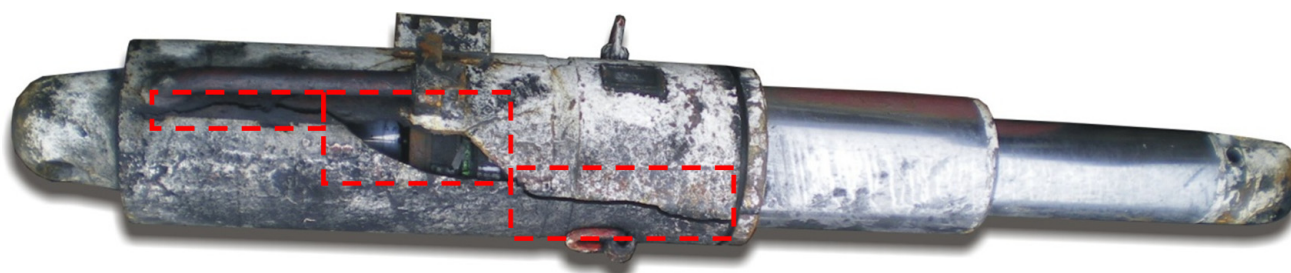
Figure 1. Area of a damaged hydraulic leg cylinder structure of a powered roof support.

The main task of a powered roof support is to maintain the roof above the workings, i.e., to provide resistance to the rock mass compressing the mine workings. Its construction has a certain load-bearing capacity, and it must be equipped with a safety valve that is placed in the construction of the hydraulic leg. The safety valve determines the behaviour of the powered roof support [33]. In a longwall system, powered roof supports play a special role, namely, the roof support set. This is because the support consists of so-called sections, which are repetitive units set along the wall with a specific pitch, most often 1.5 m. Thus, a set of supports in a wall may consist of one hundred and several dozen to two hundred sections. The support section consists of such basic elements and assemblies as the feller plate, which forms its base, the roof support floor, the hydraulic support system with hydraulic legs, and the sliding system (Figure 2).

Studies on the dynamics of hydraulic cylinders of powered roof supports can be found in the literature [34–42]. The research is based on the hydroelasticity theory taking into account the coupling between the cylinder–liquid–piston system. On the basis of this model, the problems of harmonic vibrations under force and kinematic excitation were solved. The result of this research was to determine the actual dynamics, which was proven. The study of the magnitude and nature of dynamic loads resulting from the impact of rock mass as tremors directly on powered roof supports has been the subject of numerous studies [43–48]. Many researchers from all over the world are conducting studies to identify the required dynamic resistance of the leg [49–53].

The mining exploitation in the conditions of tremor hazard sets high requirements for the producers of powered roof supports in the process of designing and testing in the test legs [54]. A powered roof support must be secured in such a way that it will not be damaged by a dynamic load. The hydraulic leg analysed in the publication had sufficient power to carry the dynamic load. The prepared leg for bench testing was used in longwalls exploited in conditions of tremor hazard (Table 1). It is on the basis of laboratory tests that it is explained how it develops its power.

The aim of this article is to propose a methodology based on bench testing to determine how much power a hydraulic leg develops as a result of dynamic loading.
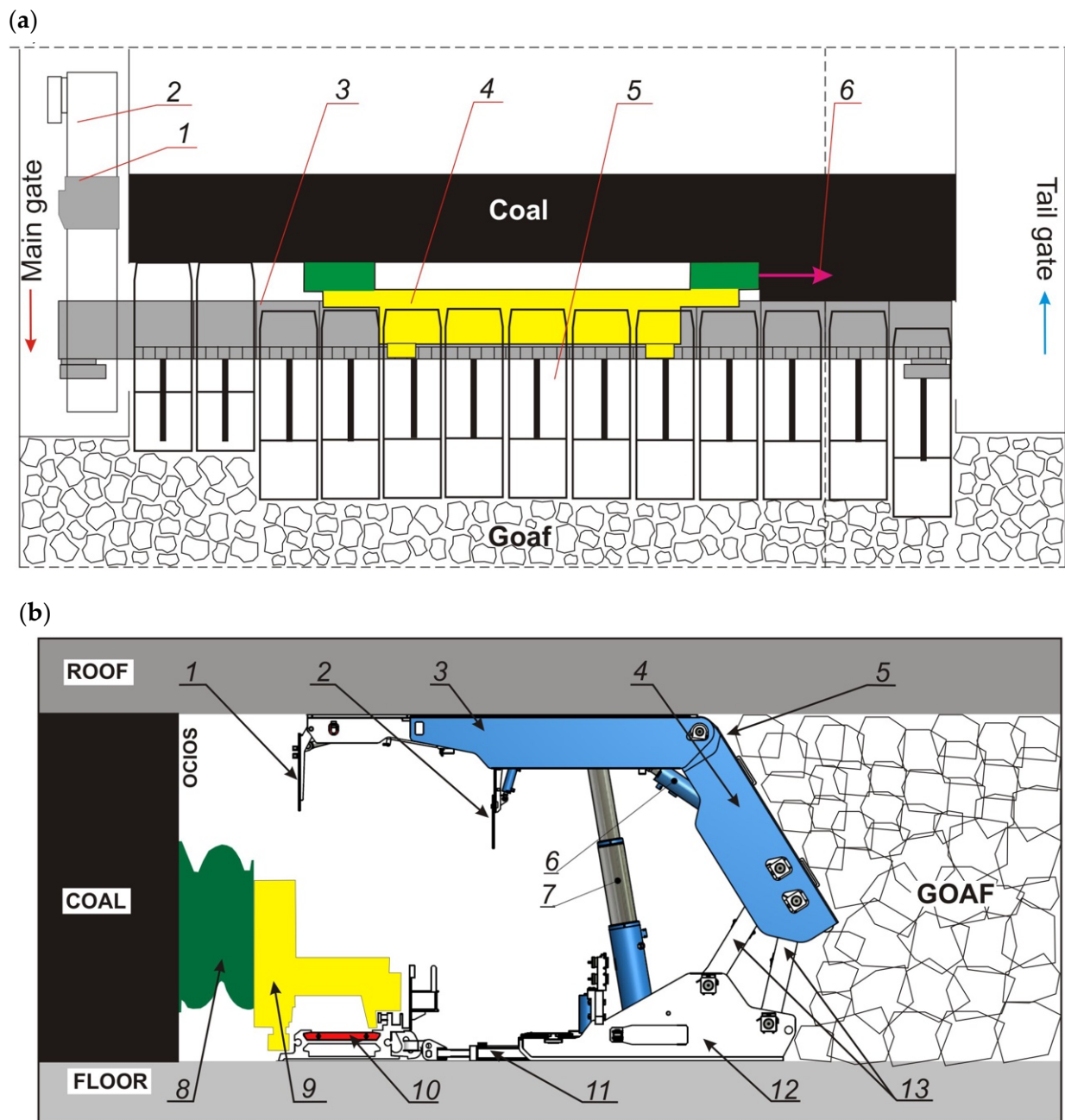
Figure 2. Example of arrangement of basic machinery of a longwall set: (**a**) longitudinal section of a longwall, where: 1—crusher, 2—main gate conveyor, 3—longwall conveyor (chock), 4—longwall shearer, 5—powered roof support, 6—mining direction; (**b**) cross-section of a longwall, where: 1—face shield, 2—transition shield, 3—canopy, 4—shield support, 5—powered roof support, 6—hydraulic support actuator, 7—hydraulic leg, 8—shearer loader, 9—shearer loader, 10—armoured face conveyor, 11—traverse system, 12—floor base, 13—linkage system.

Table 1. Calculation results for the real conditions analysed.

Longwall No.	Seam	E_p (J)	$V_{gmax(p)}$ (m/s)	Estimated Evaluation Based on the Power Method	E_p (J)	$V_{gmax(rz)}$ (m/s)	Actual Evaluation Based on the Power Method
1J	504 J	1.5×10^5	0.2	$N_{maxstoj} > D_{max\ gór}$	5×10^6	0.2	$N_{maxstoj} > D_{max\ gór}$
6	409	1.28×10^4	0.1	$N_{maxstoj} > D_{max\ gór}$	6×10^6	0.2	$N_{maxstoj} > D_{max\ gór}$
2J	504 J	9×10^7	0.2	$N_{maxstoj} > D_{max\ gór}$	5×10^6	0.2	$N_{maxstoj} > D_{max\ gór}$
3Jd	502 J	9×10^6	0.2	$N_{maxstoj} > D_{max\ gór}$	6×10^6	0.2	$N_{maxstoj} > D_{max\ gór}$
1	510 K	9×10^5	0.1	$N_{maxstoj} > D_{max\ gór}$	6×10^6	0.2	$N_{maxstoj} > D_{max\ gór}$

Note: E_p—predicted tremor energy, $V_{gmax(p)}$—predicted maximum pit clamping speed, $V_{gmax(rz)}$—actual maximum pit clamping speed, E_{rz}—actual tremor energy.

2. Materials and Methods

The basic element of a powered roof support is the hydraulic leg. It is located between the canopy and the floor base. In its sub-piston space, there is a fluid under operating pressure. When the pressure of the rock mass on the leg is constant, the working pressure is also constant. If the rock mass exerts pressure on the leg, the working pressure in its sub-piston space begins to rise until the fluid reaches the nominal pressure. The resulting pressure due to the dynamic action can lead to the destruction of the leg. For this reason, a safety valve is used for protection. Its function is to secure the under-piston space in a way that drops some of the hydraulic medium from this space to the outside. The leg is slid so that the pressure of the fluid in the sub-piston space does not rise above the nominal pressure.

2.1. Calculation Model for Actual Conditions

The power exerted by the rock mass on the leg can be calculated by knowing the speed of the force exerted on the leg and the speed of clamping the excavation using the following formula [55]:

$$N(t) = f(t)*V(t) \tag{1}$$

where:

N(t)—the power of the rock mass;
f(t)—the time course of the dynamic force acting on the support;
V(t)—the dynamic process of clamping the workings;
*—the intertwining of two time functions.

The calculation of the variation of the leg power waveform by means of Formula (1) is very difficult due to the impossibility of obtaining the corresponding variation of the leg load waveform in time as well as the pit clamping speed and the calculation of the combination of the two time functions. Based on the literature [55,56], it can be suggested that the computation of the function weave is a very complicated procedure. For the end case, i.e., the occurrence of a rockburst, the maximum power is determined by multiplying the maximum force on the leg by the maximum speed of clamping.

Ensuring safe operation of a powered roof support during strong dynamic phenomena may be achieved if the permissible load of the hydraulic leg is higher than the expected load of the leg as a result of the impact of the rock mass, which is described by the following relation:

$$N_{max\ stoj} > D_{max\ gór},\ N \cdot m \cdot s^{-1} \tag{2}$$

where:

$N_{max\ stoj}$—the maximum leg power, $N \cdot m \cdot s^{-1}$;
$D_{max\ gór}$—the maximum power that the rock mass will exert on the support, $N \cdot m \cdot s^{-1}$.

$$D_{max\ gór} = F_{gmax} \cdot V_{gmax},\ N \cdot m \cdot s^{-1} \tag{3}$$

where:

F_{gmax}—the maximum value of dynamic force applied to a single leg, N;
V_{gmax}—the maximum clamping speed of the excavation, $m·s^{-1}$.

The maximum permissible load on the leg will be calculated for the case when the workings are clamped, and there is an outflow of fluid from the working space of the leg through the safety valve. Based on the relationships described in hydromechanics and technical parameters, the leg load can be determined using the following formula:

$$N_{max\ stoj} = Q_{zaw}·k_p·P_{max},\ N·m·s^{-1} \tag{4}$$

where:

Q_{zaw}—the volume flow of the safety valve for a given pressure, $m^3·s^{-1}$;
P_{max}—the maximum working pressure of the leg matching the adopted allowable load-bearing capacity of the leg, N;
k_p—the leg's overload coefficient.

Introducing Equation (2) into Equations (3) and (4), the result is:

$$Q_{zaw}·k_p·P_{max} > F_{gmax}·V_{gmax}\ N·m·s^{-1} \tag{5}$$

By determining the minimum value of the flows using Equation (5), it is possible to achieve a fluid discharge within the safe range for the operation of the support. This value is expressed by the following formula:

$$Q_{zaw} \geq F_{gmax}·V_{gmax}/P_{max}·k_p\ (m^3·s^{-1}) \tag{6}$$

2.2. Calculation Model for Test Conditions

The kinetic energy created by a moving rock mass is proportional to the mass and the square of the velocity. The velocity of the moving rock mass is very low, on the order of a few millimetres per hour, and the kinetic energy of the rock mass is also very low. This energy is transformed into the work of sliding the powered roof support, the slide being caused mainly by the opening of the safety valve built into the hydraulic leg. For bench conditions, the mass impactor was taken as the load [25]. The leg of the support slides by conducting work that can be calculated using the following formula:

$$\varphi = P·\pi d^2/4·h_c\ (m) \tag{7}$$

where:

φ—the total work of the leg slide in the moment of dynamic loading;
P—the nominal pressure;
d—the internal diameter of the hydraulic leg cylinder;
h_c—the total leg slide in the moment of dynamic loading.

Dynamic power arises over a period of time, limited by a beginning and an end. The time in which power is created is a process of combining force and speed. Power, in this case, is defined as the energy gained over time. According to the above assumptions, this process occurring as a result of the dynamic action on the hydraulic leg will be determined by the following formula:

$$\varepsilon = E/t = \varphi/t = \delta·h_c/t\ (W) \tag{8}$$

where:

ε—the dynamic power occurring in the piston sub-space of the leg;
E—the value of kinetic energy converted by the leg;
φ—the total work of the leg slide in the moment of dynamic loading;
h_c—the total leg slide in the moment of dynamic loading;
t—the time taken for the total leg slide of h_c;
δ—the hydraulic force acting on the piston of the leg at the moment of its retraction.

3. Conducted Tests

The dynamic load on the hydraulic leg of a powered roof support is characterised by high power. The energy loading the leg is transferred to the work of sliding that leg, provided that the resulting power of the leg is at least equal to the power of its load. For safe operation, the leg power should be greater than the load power. From Equations (2) and (8), we conclude that as the load period becomes shorter, the more powerful the leg must be. Consequently, a leg operating under the tremor hazard of a rock mass has to have significantly more power than the impact of the rock mass.

In bench tests, we observe the power generated as a result of dynamic loading that occurs through the work of the leg slide. In this case, we are dealing with two relations: the slide, which is the result of elastic deformation of the stator cylinder, and the slide, which is the opening of the safety valve protecting the stator sub-piston space. Very often, these two power cases occur together, and their sum is called total power. The slide that takes place during the arising power is called the total slide, and the work conducted during this slide is called total leg slide work. There may be cases during which there is a power of energy in the hydraulic leg as a result of the opening of the leg safety valve or a load as a result of elastic deformation of the leg cylinder (short-term dynamic load in which the leg safety valve fails to open) [25].

3.1. Test Bench Model

In bench tests, when a dynamic load is applied to the leg, a rapid increase in fluid pressure is observed in its sub-piston space. This may affect the enlargement of the diameter of the leg cylinder within the elastic limit, but this issue is not being tested. The load results in a leg slide. Figure 3 shows the research model adopted. In Figure 3a, the green colour indicates the fluid pressure before the load, while Figure 3b shows the leg slide and the increase in liquid pressure indicated in red.
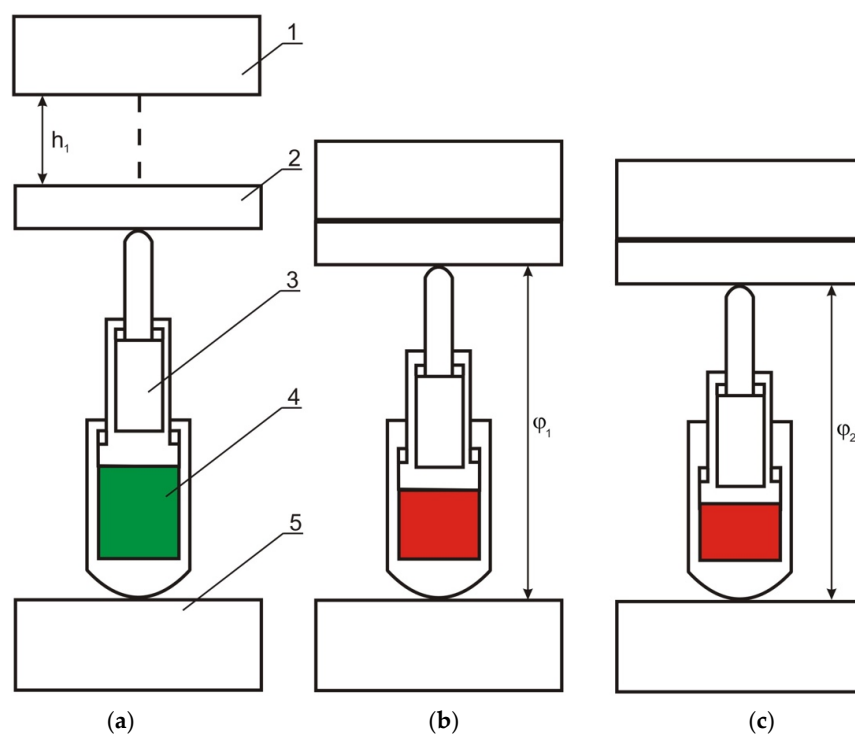
Figure 3. Schematic of the test model: (**a**) position of the leg before loading, where: 1—impact mass of the traverse m_1, 2 h_1—height for the falling mass, mass of the traverse m_2, 3—hydraulic leg, 4—working pressure, 5—foundation of the stand; (**b**) dynamic increase in fluid pressure, where φ_1—the first slide of the leg, (**c**) final increase in fluid pressure, where φ_2—the second slide of the leg.

In the process of the dynamic loading of the leg, there is a change in the fluid pressure in its sub-piston space (Figure 3). The characteristic elements of these changes are two fluid pressure increments, namely, dynamic fluid pressure increase (Figure 3b) and dynamic final fluid pressure increase (Figure 3c).

3.2. Bench Tests

According to the presented scheme (Figure 3), the test consisted of dynamically loading a hydraulic leg with an inner diameter of Ø 240 mm with a safety valve, an impact mass falling from a specified height, and a traverse of a specified mass resting on the leg. The impact weight was 20,000 kg and the traverse weight was 1800 kg. An example test for an impact mass drop height of 0.9 m is shown in Figure 4.
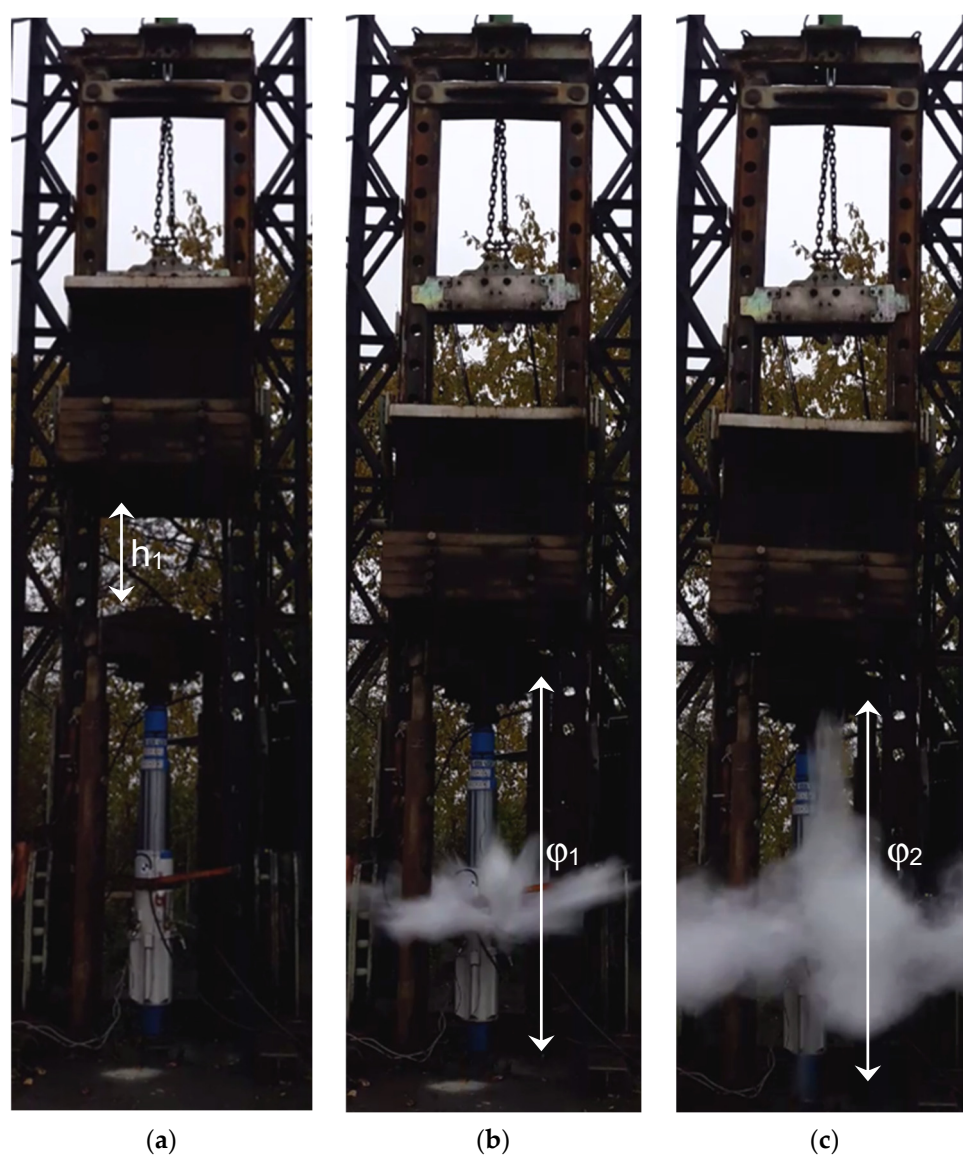
Figure 4. Testing of leg including safety valve (**a**) drop height h_1 = 0.9 m; (**b**) first chute $\varphi 1$ under dynamic load; (**c**) second slide $\varphi 2$ of the leg for final pressure build-up.

4. Results and Discussion

Based on the presented computational model for the predicted and real conditions, leg power was analysed. Based on the tremor energy, the velocity of movement of rock mass was assumed. The analysis referred to the longwalls in the Śląsk coalmine in which the

powered roof supports operated. Based on the mining and geological conditions analysed, the results are presented in Table 1.

On the basis of the analysis carried out (Table 1) for five different longwalls in which the powered roof support operated, it can be concluded that the leg had an adequate reserve of operational safety.

In the bench test, taking the working pressure as the initial stage (Figures 3a and 4a), the power under consideration starts as a result of the dynamic loading (Figures 3b and 4b). In contrast, the slide under study starts at the level of the maximum pressure obtained, as the working pressure increases in the sub-piston space of the leg due to the dynamic load on the leg. Consequently, there is leg slide caused by the displacement of the impact mass. Figure 5 shows the maximum increase in working pressure loaded with an impact mass from a height of approximately 0.9 m.
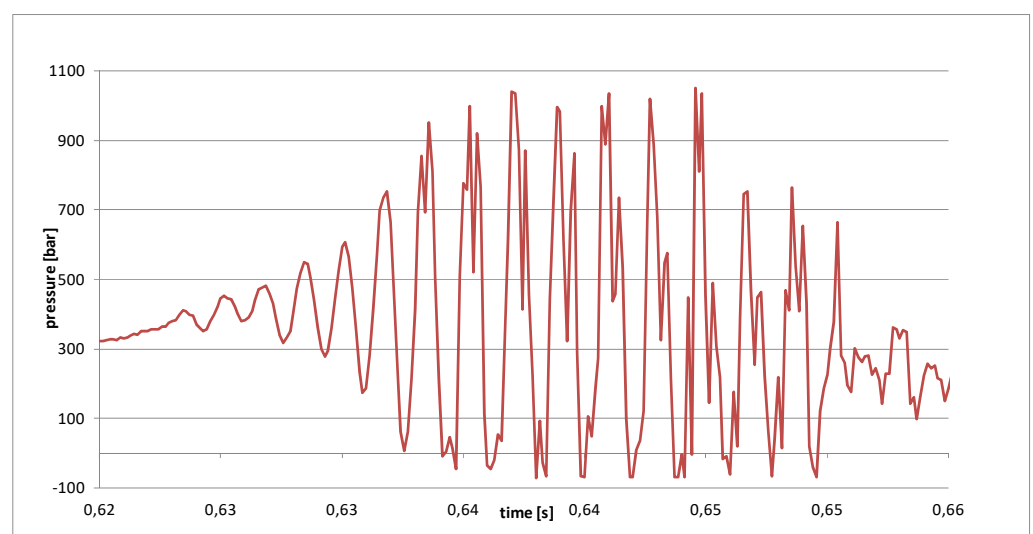
Figure 5. The resulting course of maximum fluid pressure in the sub-piston space.

The dynamic increase in pressure of the liquid in the piston cavity of the leg (Figure 5) refers to the value of the generated power as a function of the operating pressure. The dynamic increase in fluid pressure resulted in an increase in the energy loading on the leg cylinder at the time of the dynamic pulse.

In the case analysed (Figure 5), the obtained dynamic impulse lasted several tenths of a millisecond, which caused the opening of the safety valve protecting the sub-piston space. As a result, the leg slid down. The resulting dynamic pulse under bench test conditions was a high-power pulse, characterised by high kinetic energy.

During the time period indicated in the diagram (Figure 7) by the segment (*a1*), the hydraulic leg of a powered roof support is stretched in the test stand (Figures 3 and 4). It is loaded with the mass of the traverse resting on it as the fluid pressure in its sub-piston space equals the working pressure (P_{rob1}). The resulting dynamic impulse as a result of the drop in rock mass takes place at time (a_2). After time (t_2) from the occurrence of the impulse, the fluid pressure in the sub-piston space increases to the value (P_{max}), as further illustrated in Figure 8. Immediately after the activation of the dynamic impulse, the pressure of the fluid in this space decreases to the value of the working pressure (P_{rob2}) and remains at this level during the time (a_3) that the safety valve operates (Figure 6). It is only when the safety valve is opened that the pressure of the fluid in the piston cavity of the leg drops to the nominal pressure (P_{nom}). The figure also illustrates the dynamic increase in fluid pressure (a) and the dynamic increase in final fluid pressure (b). The value of the obtained power for different impact mass drop heights is shown in Table 2.

Table 2. Power occurring in the hydraulic leg during dynamic loading.

Height of Drop (m)	Energy of Impact Mass E_u (kJ)	Maximum Pressure (bar)	Leg Slide (m)	Power of the Leg (W)
0.3	58.8	550	0.03	0.5
0.4	78.4	650	0.04	0.7
0.5	98.1	730	0.05	0.9
0.6	117.7	790	0.06	1.1
0.7	137.3	830	0.08	1.3
0.8	156.9	900	0.08	1.5
0.9	176.5	990	0.09	1.7
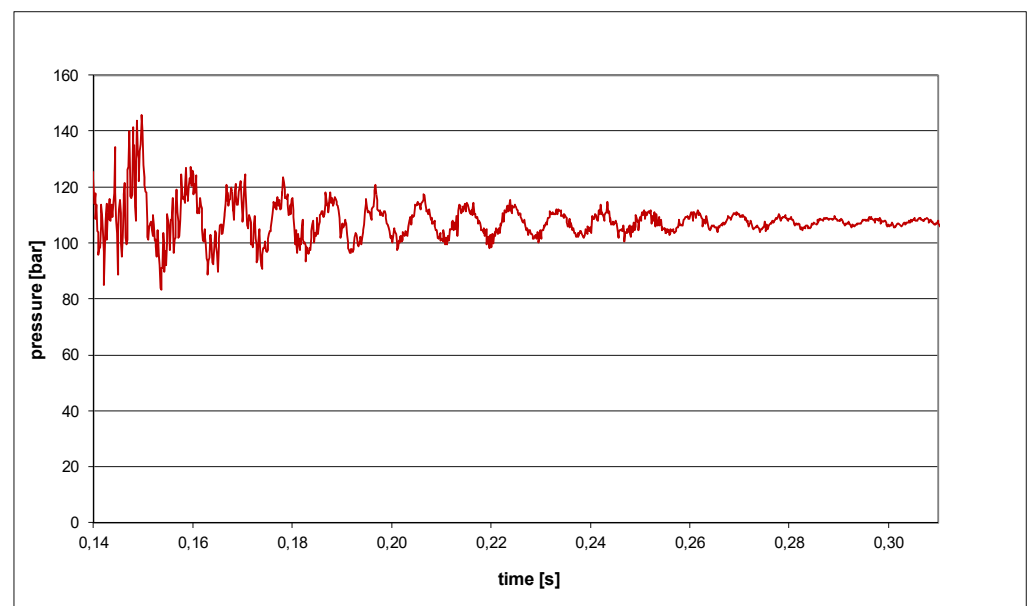
Figure 6. Opening of the safety valve.
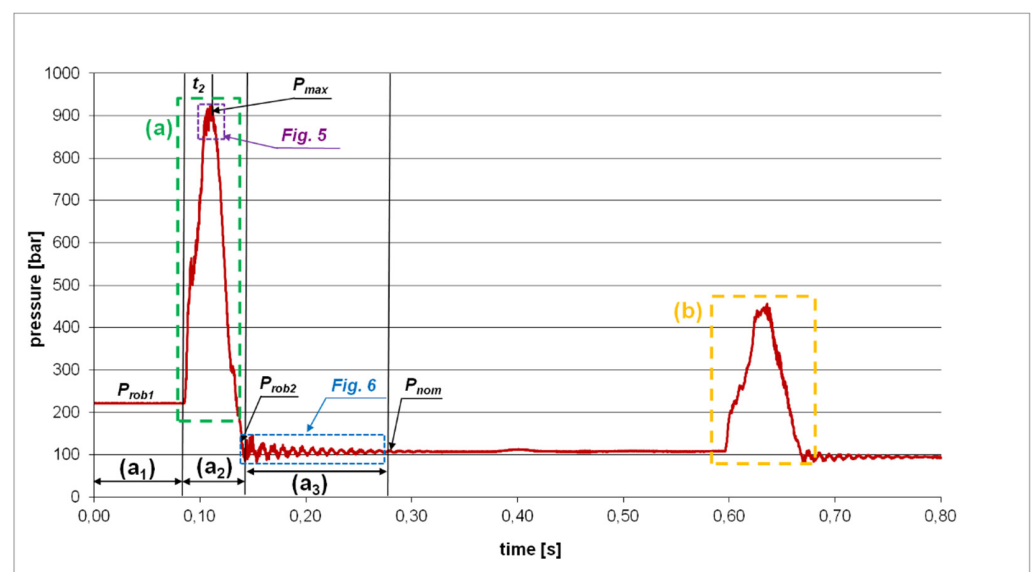
Figure 7. The course of the increase in fluid pressure for power in a specified time in the sub-piston space of a leg when it is loaded with a mass impact.
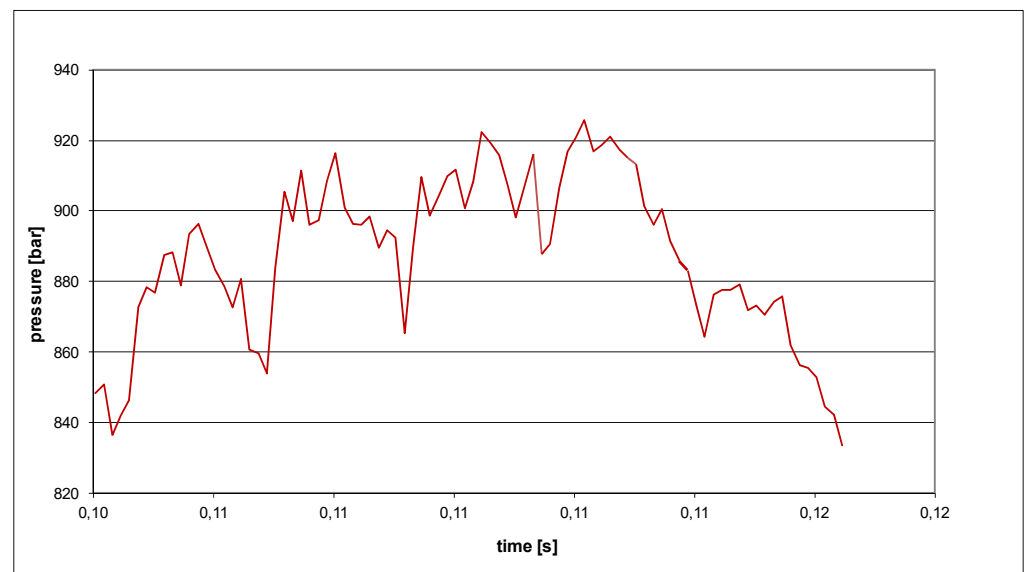
Figure 8. Increase in fluid pressure under load in progress.

5. Conclusions

The power developed by the casing must be greater than the power developed by the rock mass as a result of the tremor (Table 1). In order not to be destroyed, the powered roof support has to have greater power than the power of the rock mass. As a result of the transfer of energy from the rock mass to the powered roof support, the hydraulic legs of the support perform a slide action during the specified time in which the load energy is transferred to the powered roof support. If the powered roof support develops less power than the power developed by the rock mass, it will be damaged or destroyed. On the basis of the data (Table 1), the power of the hydraulic leg of a powered roof support operating under tremor hazard conditions was determined as well as the power that the rock mass has at the moment of the tremor.

Thirty bench tests were performed, and the tests consisted of loading the leg with an impact mass falling from a specified height (Figure 4). Each test was performed three times for a specified height of drop of the impact mass. The height of the fall in the first test was assumed to be 10 cm. For each height, three trials were carried out. The height of mass drop after three trials was increased by 10 cm. The test stand and the technical capabilities of the hydraulic leg allowed us to obtain the maximum height of mass drop to 100 cm. The paper discusses the result of the obtained test for the impact mass drop (Figure 5) from the height of 0.9 m.

When the mass impact loads the leg, it performs the work of sliding (φ), which is given by Equation (7). In the diagram (Figure 5), we have marked (a) the section in which the work of sliding is produced (φ). The resulting value of the chute work (φ) is equal to the value of the kinetic energy imparted to the leg at the time of impact. In tests, the leg was not damaged or destroyed. In contrast, if the work of the slide is less than the energy of the load, the leg could be damaged or destroyed. That is, one can conclude that if the energy created was not converted into work of the chute (φ), we would not have obtained the required leg power. The greater the sliding work (φ) a hydraulic leg can carry out, the greater the power it can achieve and the greater its resistance to dynamic loads.

The methodology presented assumes dynamic impact loading of the mass to obtain the required hydraulic leg power. This assumption makes it possible to qualify the suitability of the structure for the occurring cases of dynamic loading of the roof support's leg as a result of a rockburst. However, the research analysis presented here does not exhaust the issue of dynamic loads and only reflects the current state of knowledge and research capabilities. It is advisable to carry out further research under real and bench conditions.

References

1. Szurgacz, D.; Zhironkin, S.; Cehlár, M.; Vöth, S.; Spearing, S.; Liqiang, M. A Step-by-Step Procedure for Tests and Assessment of the Automatic Operation of a Powered Roof Support. *Energies* **2021**, *14*, 697. [CrossRef]
2. Bortnowski, P.; Gładysiewicz, L.; Król, R.; Ozdoba, M. Energy Efficiency Analysis of Copper Ore Ball Mill Drive Systems. *Energies* **2021**, *14*, 1786. [CrossRef]
3. Bajda, M.; Hardygóra, M. Analysis of Reasons for Reduced Strength of Multiply Conveyor Belt Splices. *Energies* **2021**, *14*, 1512. [CrossRef]
4. Wodecki, J.; Góralczyk, M.; Krot, P.; Ziętek, B.; Szrek, J.; Worsa-Kozak, M.; Zimroz, R.; Śliwiński, P.; Czajkowski, A. Process Monitoring in Heavy Duty Drilling Rigs—Data Acquisition System and Cycle Identification Algorithms. *Energies* **2020**, *13*, 6748. [CrossRef]
5. Ziętek, B.; Banasiewicz, A.; Zimroz, R.; Szrek, J.; Gola, S. A Portable Environmental Data-Monitoring System for Air Hazard Evaluation in Deep Underground Mines. *Energies* **2020**, *13*, 6331. [CrossRef]
6. Borkowski, P.J. Comminution of Copper Ores with the Use of a High-Pressure Water Jet. *Energies* **2020**, *13*, 6274. [CrossRef]
7. Tutak, M.; Brodny, J.; Szurgacz, D.; Sobik, L.; Zhironkin, S. The Impact of the Ventilation System on the Methane Release Hazard and Spontaneous Combustion of Coal in the Area of Exploitation—A Case Study. *Energies* **2020**, *13*, 4891. [CrossRef]
8. Góralczyk, M.; Krot, P.; Zimroz, R.; Ogonowski, S. Increasing Energy Efficiency and Productivity of the Comminution Process in Tumbling Mills by Indirect Measurements of Internal Dynamics—An Overview. *Energies* **2020**, *13*, 6735. [CrossRef]
9. Sofranko, M.; Khouri, S.; Vegsoova, O.; Kacmary, P.; Mudarri, T.; Koncek, M.; Tyulenev, M.; Simkova, Z. Possibilities of Uranium Deposit Kuriskova Mining and Its Influence on the Energy Potential of Slovakia from Own Resources. *Energies* **2020**, *13*, 4209. [CrossRef]
10. Sivák, P.; Tauš, P.; Rybár, R.; Beer, M.; Šimková, Z.; Baník, F.; Zhironkin, S.; Čitbajová, J. Analysis of the Combined Ice Storage (PCM) Heating System Installation with Special Kind of Solar Absorber in an Older House. *Energies* **2020**, *13*, 3878. [CrossRef]
11. Zhironkin, S.; Selyukov, A.; Gasanov, M. Parameters of Transition from Deepening Longitudinal to Continuous Lateral Surface Mining Methods to Decrease Environmental Damage in Coal Clusters. *Energies* **2020**, *13*, 3305. [CrossRef]
12. Beer, M.; Rybár, R.; Cehlár, M.; Zhironkin, S.; Sivák, P. Design and Numerical Study of the Novel Manifold Header for the Evacuated Tube Solar Collector. *Energies* **2020**, *13*, 2450. [CrossRef]
13. Kawalec, W.; Suchorab, N.; Konieczna-Fuławka, M.; Król, R. Specific Energy Consumption of a Belt Conveyor System in a Continuous Surface Mine. *Energies* **2020**, *13*, 5214. [CrossRef]
14. Szrek, J.; Wodecki, J.; Błażej, R.; Zimroz, R. An Inspection Robot for Belt Conveyor Maintenance in Underground Mine—Infrared Thermography for Overheated Idlers Detection. *Appl. Sci.* **2020**, *10*, 4984. [CrossRef]
15. Kozłowski, T.; Wodecki, J.; Zimroz, R.; Błażej, R.; Hardygóra, M. A Diagnostics of Conveyor Belt Splices. *Appl. Sci.* **2020**, *10*, 6259. [CrossRef]
16. Schmidt, S.; Zimroz, R.; Chaari, F.; Heyns, P.S.; Haddar, M. A Simple Condition Monitoring Method for Gearboxes Operating in Impulsive Environments. *Sensors* **2020**, *20*, 2115. [CrossRef]
17. Hebda-Sobkowicz, J.; Zimroz, R.; Wyłomańska, A. Selection of the Informative Frequency Band in a Bearing Fault Diagnosis in the Presence of Non-Gaussian Noise—Comparison of Recently Developed Methods. *Appl. Sci.* **2020**, *10*, 2657. [CrossRef]
18. Sobik, L.; Brodny, J.; Buyalich, G.; Strelnikov, P. Analysis of methane hazard in longwall working equipped with a powered longwall complex. *E3S Web Conf.* **2020**, *174*, 1011. [CrossRef]
19. Brodny, J. Determining the working characteristic of a friction joint in a yielding support. *Arch. Min. Sci.* **2010**, *55*, 733–746.
20. Brodny, J. Tests of Friction Joints in Mining Yielding Supports Under Dynamic Load. *Arch. Min. Sci.* **2011**, *56*, 303–318.
21. Budirskỳ, S. Interaction of powered supports and the strata in coal seams under a heavy roof. *Int. J. Min. Eng.* **1985**, *3*, 113–138. [CrossRef]
22. Szurgacz, D.; Brodny, J. Analysis of the Influence of Dynamic Load on the Work Parameters of a Powered Roof Support's Hydraulic Leg. *Sustainability* **2019**, *11*, 2570. [CrossRef]
23. Stoiński, K.; Mika, M. Dynamics of Hydraulic Leg of Powered Longwall Support. *J. Min. Sci.* **2003**, *39*, 72–77. [CrossRef]
24. Szweda, S. Dynamic action of rock mass on the powered support legs. *J. Min. Sci.* **2003**, *38*, 154–161. [CrossRef]
25. Gwiazda, J.B. *Górnicza Obudowa Hydrauliczna Odporna na Tąpania*; Wydawnictwo Śląsk: Katowice, Poland, 1997.
26. Budirskỳ, S.; Martinec, P. Influence of support resistance on roof control in single-pass thick-seam mining (4.5 m): A case history. *Min. Sci. Technol.* **1986**, *4*, 59–67. [CrossRef]
27. Klishin, V.I.; Klishin, S.V. Coal Extraction from Thick Flat and Steep Beds. *J. Min. Sci.* **2010**, *46*, 149–159. [CrossRef]

28. Buyalich, G.; Buyalich, K.; Byakov, M. Factors Determining the Size of Sealing Clearance in Hydraulic Legs of Powered Supports. *E3S Web Conf.* **2017**, *21*, 3018. [CrossRef]

29. Buyalich, G.; Byakov, M.; Buyalich, K. Factors Determining Operation of Lip Seal in the Sealed Gap of the Hydraulic Props of Powered Supports. *E3S Web Conf.* **2017**, *41*, 1045. [CrossRef]

30. Buyalich, G.; Byakov, M.; Buyalich, K.; Shtenin, E. Development of Powered Support Hydraulic Legs with Improved Performance. *E3S Web Conf.* **2019**, *105*, 3025. [CrossRef]

31. Kabiesz, J.; Konopko, W.; Patyńska, R. *Annual Report on the State of Basic Natural and Technical Hazards in Hard Coal Mining*; GIG: Katowice, Poland, 2020; pp. 97–101.

32. Stoiński, K. *Mining Roof Support in Hazardous Conditions of Mining Tremors*; The Central Mining Institute: Katowice, Poland, 2000.

33. Świątek, J.; Janoszek, T.; Cichy, T.; Stoiński, K. Computational Fluid Dynamics Simulations for Investigation of the Damage Causes in Safety Elements of Powered Roof Supports—A Case Study. *Energies* **2021**, *14*, 1027. [CrossRef]

34. Tomski, L.; Kukla, S. Dynamical response of bar-fluid-shell system simulating hydraulic cylinder subjected to arbitrary axial excitation. *J. Sound Vib.* **1984**, *92*, 273–284. [CrossRef]

35. Tomski, L.; Uzny, S. A hydraulic cylinder subjected to Euler's load in aspect of the stability and free vibrations taking into account discrete elastic elements. *Arch. Civ. Mech. Eng.* **2011**, *11*, 769–785. [CrossRef]

36. Sochacki, W.; Tomski, L. Free Vibration and Dynamic Stability of a Hydraulic Cylinder Set. *Mach. Dyn. Probl.* **1999**, *23*, 91–104.

37. Tomski, L. Forced Vibrations of Hydraulic Props of Longwall Supports. *Arch. Min. Sci.* **1979**, *24*, 19–33.

38. Tomski, L. *Dynamika Stojaków Hydraulicznych Obudów Górniczych*; Zeszyty Naukowe Politechniki Częstochowskiej, Nr 17; Politechnika Częstochowska: Częstochowa, Poland, 1979.

39. Tomski, L. Elastic Carrying Capacity of a Hydraulic Prop. *Eng. Trans.* **1977**, *25*, 247–263.

40. Tomski, L. Elastic Stability of Hydraulic Props of Longwall Supports. *Arch. Min. Sci.* **1978**, *23*, 217–231.

41. Tomski, L. Longitudinal Mass Impact of Hydraulic Servo. *Z. Angew. Math. Mech.* **1981**, *61*, 191–193.

42. Tomski, L.; Chwalba, W.; Kukla, S.; Mrowiec, A.; Posiadała, B. Dynamical Response of Hydraulic Cylinder Connected with External Shock Absorber Subjected to Axial Mass Impact. *Arch. Min. Sci.* **1987**, *32*, 439–454.

43. Yang, Z.K.; Sun, Z.Y.; Jiang, S.B.; Mao, Q.H.; Liu, P.; Xu, C.Z. Structural Analysis on impact-mechanical properties of ultra-high hydraulic support. *Int. J. Simul. Model* **2020**, *1*, 17–28. [CrossRef]

44. Uzny, S. Free Vibrations of an Elastically Supported Geometrically Nonlinear Column Subjected to a Generalized Load with a Force Directed toward the Positive Pole. *J. Eng. Mech.* **2011**, *137*, 740–748. [CrossRef]

45. Uzny, S.; Osadnik, M. Influence of longitudinal elastic support on stability of a partially tensioned column. In Proceedings of the 23rd International Conference in Engineering Mechanics, Svratka, Czech Republic, 15–18 May 2017; pp. 1006–1009.

46. Uzny, S.; Kutrowski, Ł. Strength analysis of a telescopic hydraulic cylinder elastically mounted on both ends. *J. App. Math. Comput. Mech.* **2019**, *18*, 89–96. [CrossRef]

47. Uzny, S.; Kutrowski, Ł. The Effect of the Type of Mounting on Stability of a Hydraulic Telescopic Cylinder. *Mach. Dyn. Res.* **2018**, *42*, 53–60.

48. Uzny, S. Free vibrations and stability of hydraulic cylinder fixed elastically on both ends. *Proc. Appl. Math. Mech.* **2009**, *9*, 303–304. [CrossRef]

49. Kong, D.Z.; Jiang, W.; Chen, Y. Study of roof stability of the end of working face in upward longwall top coal. *Arab. J. Geosci.* **2017**, *10*, 185. [CrossRef]

50. Michalak, M. Gradual-Randomized model of powered roof supports working cycle. *Comput. Sci. Inform. Technol.* **2015**, 15–24. [CrossRef]

51. Axin, M. Mobile Working Hydraulic System Dynamics. Ph.D. Thesis, Linköping Studies in Science and Technology, Linköping University, Linköping, Sweden, 2015.

52. Brady, B.H.G.; Brown, E.T. *Rock Mechanics for Underground Mining*; Kluwer Academic Publishers: New York, NY, USA, 2005.

53. Singh, R.; Singh, T.N. Investigation into the behavior of a support system and roof strata during sublevel caving of a thick coal seam. *Geotech. Geol. Eng.* **1999**, *17*, 21–35. [CrossRef]

54. Gil, J.; Kołodziej, M.; Szurgacz, D.; Stoiński, K. Introduction of standardization of powered roof supports to increase production efficiency of Polska Grupa Górnicza, S.A. *Min. Inform. Autom. Electr. Eng.* **2019**, *56*, 33–38. [CrossRef]

55. Szurgacz, K. An attempt to determine the dynamic powered of mechanized longwall housing leg deisgned to work in hazardous conditions of rock mass tremors—Discussion article. *Res. Rep. Min. Environ.* **2011**, *1*, 79–88.

56. Stoiński, K. *Powered Roof Support for Rock Tremors Conditions*; The Central Mining Institute: Katowice, Poland, 2018.